RESEARCH ARTICLE

Alzheimer's & Dementia®
THE JOURNAL OF THE ALZHEIMER'S ASSOCIATION

APOE ε4-related blood–brain barrier breakdown is associated with microstructural abnormalities

Emilie T. Reas[1] 🟢 | **Seraphina K. Solders[1]** | **Amaryllis Tsiknia[2]** | **Curtis Triebswetter[3]** | **Qian Shen[1]** | **Charlotte S. Rivera[1]** | **Murray J. Andrews[4]** | **Austin Alderson-Myers[1]** | **James B. Brewer[1,5]**

[1]Department of Neurosciences, University of California, San Diego, La Jolla, California, USA

[2]Imaging Genetics Center, USC Mark and Mary Stevens Neuroimaging and Informatics Institute, Marina Del Rey, California, USA

[3]University of Arizona College of Medicine - Phoenix, Phoenix, Arizona, USA

[4]Boston University Chobanian and Avedisian School of Medicine, Boston, Massachusetts, USA

[5]Department of Radiology, University of California, San Diego, La Jolla, California, USA

Correspondence
Dr. Emilie T. Reas, Department of Neurosciences, Mail code 0841, UCSD, 9500 Gilman Dr., La Jolla, CA 92093-0841, USA.
Email: ereas@health.ucsd.edu

Abstract

INTRODUCTION: Blood–brain barrier (BBB) dysfunction occurs in Alzheimer's disease (AD). Yet, the stage at which it appears along the AD time course and whether it contributes to neurodegeneration remain unclear.

METHODS: Older adults (61 to 90 years) from cognitively normal (CN) to mildly cognitively impaired (CI), enriched for APOE ε4 and amyloid positivity, underwent dynamic contrast-enhanced (DCE) magnetic resonance imaging (MRI) and diffusion MRI to measure BBB permeability and brain microstructure. Analysis of variance compared BBB permeability according to cognitive status, amyloid beta (Aβ), and APOE4. Linear regressions assessed associations of BBB permeability with brain microstructure and interactions with Aβ and APOE4.

RESULTS: BBB permeability was elevated for APOE4 carriers across the cortical gray matter, with the strongest differences among CN amyloid-negative individuals. Associations between entorhinal BBB permeability and microstructure interacted with Aβ and APOE4, with the strongest relationships in amyloid-positive individuals and APOE4 carriers.

DISCUSSION: APOE4 may drive widespread BBB dysfunction in preclinical AD, which may contribute to neurodegenerative changes early along the AD cascade.

KEYWORDS
Alzheimer's disease, amyloid, APOE, blood–brain barrier, diffusion MRI

Highlights

- Gray matter blood–brain barrier (BBB) permeability is elevated for APOE4 carriers.
- APOE4-related BBB breakdown appears in the absence of cognitive decline or amyloid.
- BBB leakage correlates with entorhinal cortex microstructural injury.
- Associations with microstructure are strongest for amyloid-positive APOE4 carriers.

1 | BACKGROUND

The blood–brain barrier (BBB) is a semi-permeable neurovascular interface that regulates transport between cerebral blood and the parenchymal extravascular space. The BBB comprises endothelial cells adjoined via tight junctions and is supported by pericytes and astrocytes, which together maintain brain homeostasis by preventing the infiltration of blood-borne toxins, selectively transporting nutrients, and facilitating waste removal. Although morphological and functional alterations to the BBB have been documented with aging, material age-related BBB breakdown has not been consistently observed in humans.[1] Molecular and neuroimaging studies have more reliably demonstrated increased BBB permeability in Alzheimer's disease (AD) and related dementias.[2,3] In light of the high prevalence of AD and other neuropathologies in cognitively intact older adults, undetected pathophysiology may significantly contribute to age-related BBB dysfunction. A central role for BBB breakdown in AD pathogenesis is supported by evidence of contributions from cerebral vessel pathology and vascular risk factors to the development and progression of AD.[4] BBB disruption may promote AD through diverse mechanisms, including infiltration of blood-borne immune signaling molecules, toxins, or pathogens, impaired nutrient delivery, or disrupted transvascular transport or paravascular glymphatic clearance of pathogenic proteins.[5]

Studies using biochemical markers of pericyte injury or blood-derived proteins in cerebrospinal fluid (CSF) have reported BBB abnormalities in mild cognitive impairment (MCI) and AD,[3,6,7] with conflicting evidence for carriers of the apolipoprotein (APOE) ε4 allele, the strongest single genetic risk factor for sporadic AD.[3,8,9] However, molecular markers are indirect and regionally non-specific measures of BBB integrity. Dynamic contrast-enhanced (DCE) magnetic resonance imaging (MRI), which exploits T_1 signal enhancement over time by a gadolinium-based contrast agent to estimate paracellular contrast leakage from intravascular to extravascular spaces, allows more direct measurement of regional neurovascular permeability. DCE MRI studies have confirmed BBB leakage in MCI and AD[10,11] and, more recently, have reported BBB breakdown in *APOE4* carriers.[12,13] While a genetic link implicates BBB dysfunction as a significant preclinical event in the AD cascade, the *APOE*-dependent mechanisms by which BBB breakdown may contribute to AD remain unclear. *APOE4* regulates diverse pathways that can influence BBB structure and function, including microglial activation and proinflammatory signaling,[14,15] vascular atrophy and vascular amyloid beta (Aβ) deposition,[16,17] tight junction disruption,[18] and altered expression and activity of barrier receptors and transporters.[19]

BBB breakdown in AD has been observed independently of Aβ and neurodegeneration using measures of macroscopic atrophy.[6] However, a potential role for BBB dysfunction in promoting neurodegeneration is supported by studies indicating correlations between CSF markers of BBB integrity and axonal damage[20] and findings from animal models that *APOE4*-mediated BBB breakdown leads to neuronal damage.[15] DCE MRI studies have observed elevated permeability with mild cognitive deficits in medial temporal regions that are susceptible

---

RESEARCH IN CONTEXT

1. **Systematic review**: The authors conducted a systematic review of peer-reviewed literature on blood–brain barrier (BBB) dysfunction in Alzheimer's disease (AD). Existing research provides evidence for BBB breakdown in early AD, limited but inconclusive support for an association between *APOE4* and BBB breakdown, and minimal examination of associations with neurodegeneration.

2. **Interpretation**: *APOE4*-related BBB dysfunction occurs across cortical gray matter, even in the absence of detectable cognitive decline or amyloid beta pathology, and is associated with microstructural injury in the entorhinal cortex, particularly for amyloid-positive *APOE4* carriers. *APOE4*-related BBB breakdown may represent an early pathophysiological event along the AD cascade that contributes to neurodegeneration.

3. **Future directions**: Future investigation is needed to clarify the mechanisms by which *APOE4* may disrupt BBB function and the avenues by which BBB dysfunction in turn promotes neurodegeneration.

---

to early tau accumulation and AD-related atrophy, including the hippocampus and parahippocampal cortex,[6] whereas others have reported widespread cortical gray matter leakage in MCI and AD.[11] Thus, considerable uncertainty remains over whether BBB dysfunction in AD originates in medial temporal targets of early AD-related neurodegeneration or emerges diffusely across the cortex, as well as over the avenues by which BBB dysfunction may drive neurodegeneration. Advanced neuroimaging approaches such as multicompartment diffusion MRI, which characterizes nuanced tissue microstructure, may help to elucidate subtle cytoarchitectural abnormalities accompanying BBB dysfunction that are not measurable using macroscopic volumetrics.

This investigation leveraged a multimodal approach combining DCE MRI and the multicompartment diffusion MRI technique restriction spectrum imaging (RSI) with genetic and Aβ characterization to understand how BBB dysfunction and associated neurodegeneration manifest along the early AD continuum. We sought to first validate prior inconclusive reports of BBB leakage among *APOE4* carriers, evaluating competing hypotheses that *APOE4*-related BBB dysfunction presented focally in regions vulnerable to early AD-related atrophy versus diffusely across cortical gray matter or white matter. To interrogate associations of BBB dysfunction with neurodegeneration, we further examined regional relationships with brain microstructure and their modification by Aβ and *APOE4*.

2 | METHODS

2.1 | Participants

Eligible participants included University of California (UC) San Diego Shiley-Marcos Alzheimer's Disease Research Center (ADRC) participants ($N = 52$) and residents of the San Diego community ($N = 9$), who completed MRI scans from December 2019 to January 2024 and had available genetic data. ADRC participants underwent clinical, neurological, and neuropsychological evaluation and consensus diagnosis of cognitively normal (CN), MCI, or AD dementia was determined by a team of two senior neurologists and a neuropsychologist, according to ADRC protocol.[21] Due to our a priori interest in preclinical AD and the effects of *APOE4*, recruitment efforts prioritized *APOE4* carriers and Aβ-positive individuals. Community participants also completed neuropsychological evaluation and were considered CN if they reported no subjective cognitive complaints and demonstrated no objective impairment on the Mini-Mental State Examination (MMSE) (community participant MMSE scores ranged from 29 to 30). Exclusion criteria included moderate to severe dementia, cognitive impairment due to non-AD etiology, history of stroke, other neurological disease, treatment for a substance use disorder, safety contraindication for MRI, history of kidney disease, glomerular filtration rate <60 mL/min/1.73 m^3, or known allergy to gadolinium-based contrast agents. Six participants were excluded from analysis for the following reasons: abnormal MRI finding ($N = 2$), prior concussion ($N = 1$), asymptomatic SARS-CoV-2 infection during MRI ($N = 1$), long COVID ($N = 1$), and uncorrectable imaging artifact ($N = 1$). MCI ($N = 9$) and mild AD ($N = 2$) were combined into a cognitively impaired (CI) group for analysis. The final sample included 55 participants (44 CN, 11 CI: 47% women; age: mean ± SD 76.2 ± 6.4, range 61 to 90 years).

2.2 | Standard protocol approvals and participant consents

Study procedures were approved by the UC San Diego Human Research Protections Program Board, and participants provided informed written consent before participation. Consent for CI participants was provided by a surrogate.

2.3 | APOE genotyping

For ADRC participants, the *APOE* genotype was provided by the National Alzheimer's Coordinating Center (NACC). For community participants, genetic sequencing was conducted on saliva samples by Diagnomics, Inc. using the Illumina V2.2 array. *APOE* genotype was determined by imputation of single-nucleotide polymorphisms rs429,358 and rs7412. Participants were classified as *APOE4* noncarriers (25 *APOE ε3ε3*) or *APOE4* carriers (two *APOE ε2ε4*, 26 *APOE ε3ε4*, two *APOE ε4ε4*).

2.4 | Determination of Aβ status

Aβ biomarkers were available on 50 participants, measured 2.1 ± 3.0 years before MRI through standard operating procedures of the UC San Diego Shiley-Marcos ADRC. [^{18}F]Florbetapir positron emission tomography (PET), available on 14 participants, was the preferred method of determining Aβ status. PET acquisition followed the National Institute on Aging (NIA) Standardized Centralized Alzheimer's & Related Dementias Neuroimaging (SCAN) protocol, with dynamic PET images (4 × 5 min frames) acquired on a GE Discovery 610 scanner 50 to 70 min after injection of 10 mCi ± 10%. Imaging data were reconstructed using iterative Vue Point HD (4 iterations × 16 subsets; 192 × 192 mm, 256 × 256 mm field of view (FOV)). Aβ positivity was determined by expert visual read by a neurologist (J.B.B.).

CSF Aβ-42/40 was the next preferred biomarker, available to 32 participants. Participants underwent lumbar puncture, as previously detailed,[22] by best practice recommendations.[23] Briefly, a neurologist collected 15 to 20 mL of CSF using a Sprotte atraumatic 24-gauge needle, in the morning after overnight fasting. Samples were gently mixed, centrifuged in a polypropylene conical tube at 1500 rpm for 10 min, aliquoted into Sarstedt 0.5-mL cryotubes, snap-frozen, and stored at −80°C until assayed. Levels of Aβ-40 and Aβ-42 were measured using either mass spectrometry (Quest Diagnostics; $N = 19$) or the automated Lumipulse platform using established monoclonal antibody assays (Fujirebio Inc.; $N = 13$). CSF samples with gross blood contamination or with red blood cell counts >10/mL were not used. Participants were classified as amyloid-positive using an Aβ-42/40 cutoff of <0.16 for Quest, shown to identify amyloid PET positivity with 90% sensitivity and specificity.[24] A cutoff of <0.056 for Lumipulse was determined from a mixture model analysis of patients versus controls across the AD continuum from the UC San Diego ADRC.

For four participants without amyloid PET or CSF data, Aβ status was inferred from plasma phosphorylated tau181 (p-tau181). The blood draw was performed by a trained phlebotomist, and blood was centrifuged at 2000 × g for 10 min at 4°C within an hour of blood draw. Plasma was separated and aliquoted into 500-μL fractions into polypropylene cryotubes (VWR or Sarstedt), snap frozen, and stored at −80°C. Plasma samples were processed by the National Centralized Repository for Alzheimer's Disease and Related Dementias (NCRAD) biomarker laboratory to measure p-tau181 using the Quanterix Simoa HDx version 2 immunoassay. A cutoff of p-tau181 > 4.09 pg/mL, which has been found to best identify Aβ PET positivity in an independent sample,[25] was used.

2.5 | Cognitive assessment

A neuropsychological test battery[26] was administered by a trained examiner in a quiet room. The MMSE is a cognitive screening tool that tests global cognition. The Trail-Making Test, Part B measures time to complete a number-sequencing task and assesses psychomotor processing speed and executive function. Animal naming evaluates verbal

semantic fluency and requires participants to name as many unique animals as possible within 1 min. The WMS-R Logical Memory subtest prompts participants to report details of a passage, immediately and after delay. The California Verbal Learning Test (CVLT) evaluates recall from a list of categorized words; this study analyzed measures of learning (Trials 1 to 5 correct) as well as immediate and delay-free recall.

2.6 | Imaging data acquisition

Imaging data were acquired on two 3.0 Tesla Discovery 750 scanners (GE Healthcare, Milwaukee, WI, USA) at the UC San Diego Center for Translational Imaging and Precision Medicine. Following a three-plane localizer, a sagittal 3D fast spoiled gradient echo (FSPGR) T_1-weighted structural scan optimized for maximum tissue contrast (echo time [TE] = 2.9 ms, repletion time [TR] = 6.7 ms, inversion time = 450 ms, flip angle = 8, FOV = 240 × 240 mm, matrix = 256 × 256, slice thickness = 1.2 mm, resampled to 1 mm^3 resolution) and an axial 2D single-shot pulsed-field gradient spin-echo echo-planar diffusion-weighted sequence (45 gradient directions, b values = 0, 500, 1500, 4000 s/mm^2, one $b = 0$ volume, and 15 gradient directions for each non-zero b value; TR = 8 s, FOV = 240 × 240 mm, matrix = 96 × 96, slice thickness = 2.5 mm, resampled to 2 mm^3 resolution) were acquired. For BBB permeability measurement, four FSPGR sequences (20 s each) with flip angles of 2, 5, 10, 15 (all other parameters equal to the subsequent DCE FSPGR) were conducted for T_1-mapping, followed by an axial DCE FSPGR sequence (flip angle = 30°, FOV = 256 × 256 mm, matrix = 256 × 256, slice thickness = 5 mm, slices = 28). Due to software upgrades, total image volumes for the DCE scan ranged from 53 to 58, TR ranged from 7.7 to 8.2 ms, and temporal resolution ranged from 18.3 to 20.3 s. After a 3-min baseline, Gadavist (gadobutrol; 0.1 mL/kg) was injected at a flow rate of 2 mL/s, followed by a 20-mL saline flush.

2.7 | Data processing

Raw and processed MRI images were visually inspected for artifacts and processed using the multimodal processing stream,[27] an automated image processing pipeline that integrates FreeSurfer and FMRIB Software Library (FSL)[28] with in-house software. FreeSurfer (version 6.0) was used to reconstruct cortical gray matter, white matter, and CSF boundaries from T_1-weighted images and automatically segment subcortical regions according to a subcortical atlas.[29] Cortical editing to remove non-brain voxels or add white matter control points was performed when deemed necessary. As previously detailed,[27] diffusion MRI data underwent eddy current correction, correction for head motion with rigid-body registration, and correction for B_0 field inhomogeneity spatial and intensity distortions. The $b = 0$ images were registered to T_1 images using mutual information and diffusion images were aligned with a fixed rotation and translation relative to the T_1 image. White matter tracts were labeled using AtlasTrack, a fiber atlas based on prior probability and orientation information,[30] and voxels containing primarily gray matter or CSF were excluded from white matter.[29] DCE FSPGR images were registered to T_1 images using mutual information co-registration in SPM12 (http://fil.ion.ucl.ac.uk/spm/).

2.8 | Computation of imaging metrics

To evaluate competing hypotheses that AD-related BBB breakdown is (1) localized to medial temporal regions demonstrating early AD-related neurodegeneration versus (2) widespread, occurring across cortical gray or white matter, imaging metrics were computed in the hippocampus, entorhinal cortex, and parahippocampal gyrus and across global gray and white matter. Measures were averaged between hemispheres and global metrics were computed as the mean signal across the FreeSurfer-derived cortical gray matter mask and AtlasTrack-derived fiber tracts, respectively.

K_{trans}, the transfer coefficient reflecting neurovascular permeability, was the pharmacokinetic measure of interest, computed from DCE MRI images in ROCKETSHIP[31] using the Patlak model, which is optimal for conditions of low permeability.[32] Hematocrit levels used for modeling were measured from blood samples collected within 6 weeks before the MRI. A vascular input function was derived from the superior sagittal sinus, recommended to reduce partial volume effects and inflow artifacts,[33] using the 3D Fill tool in MRIcron (https://www.nitrc.org/projects/mricron). On each participant's volume with peak vessel signal intensity, the origin was set in the vessel center in the posterior parietal midline region, the radius was set to 50 mm, and other settings (erode/dilate cycles, the difference from origin, difference at edge, and contrast maximum) were adjusted to ensure coverage of the sinus while avoiding pixels at the edge. Masks were examined over the entire dynamic series to ensure that they did not land outside the vessel due to motion. To exclude physiologically implausible values, K_{trans} values below 10^{-7} were set to this threshold.

Computed RSI metrics included restricted isotropic diffusion, consistent with the fraction of intracellular diffusion present in cell bodies; neurite density, anisotropic restricted diffusion consistent with neurites; hindered isotropic diffusion, non-restricted diffusion that is hindered by cellular barriers and is consistent with diffusion within large cell bodies or the extracellular space; and isotropic free water, a measure of CSF.[34] A MRI software upgrade over the study period introduced differences in computed RSI metrics, with 43 and 12 scans collected with each software version; thus, a binary covariate was included in analyses of RSI measures to account for the software version.

2.9 | Statistical analysis

Analyses were conducted in SPSS version 29.0 (IBM Corp., Armonk, NY, USA), and significance was set to $p < 0.05$. Group differences in participant characteristics were examined using two-tailed independent

TABLE 1 Participant characteristics (mean ± SD or N [%]) for all participants and by cognitive status.

	N	All N = 55	CN N = 44	CI N = 11	Group difference
Age (years)	55	76.2 ± 6.4	75.8 ± 6.3	77.8 ± 6.7	$t(53) = 0.92, p = 0.36$
Sex (women)	55	N = 26 (47%)	N = 22 (50%)	N = 4 (36%)	$x^2(1) = 0.66, p = 0.42$
Education (years)	55	17.0 ± 2.2	16.8 ± 2.2	18.0 ± 2.2	$t(53) = 1.70, p = 0.10$
APOE (33/24/34/44)[a]	55	N = 25/2/26/2 (45/4/47/4%)	N = 21/2/20/1 (48/5/45/2%)	N = 4/0/6/1 (36/0/55/9%)	$x^2(1) = 0.46, p = 0.50$
Amyloid positive	50	N = 35 (64%)	N = 26 (63%)	N = 9 (100%)	$x^2(1) = 4.70, p = 0.03$
MMSE[b]	55	28.7 ± 2.1	29.1 ± 1.4	27.4 ± 3.6	$F(1,50) = 5.88, p = 0.02$

Abbreviations: CN, cognitively normal; CI, cognitively impaired.
Bold indicates significant ($p<0.05$).
[a] x^2 value is for APOE4 carrier/non-carrier.
[b] MMSE scores are adjusted for age, sex, and education.

sample t tests for continuous variables or chi-squared tests for categorical variables. Associations of K_{trans} with age and education were examined with Pearson's correlations, and sex differences in K_{trans} were assessed using analyses of covariance (ANCOVA), covaried for age.

To assess whether BBB permeability was related to cognitive function, linear regressions were conducted with K_{trans} as the regressor, cognitive test score as the outcome, and covariates of age, sex, and years of education.

To examine differences in BBB permeability by Aβ (positive/negative) and APOE4 (carrier/non-carrier), ANCOVA was conducted with K_{trans} as the dependent variable and covariates of age and sex. To assess whether differences by APOE4 were driven by AD pathological burden, secondary models of APOE4 were further adjusted for Aβ. Although our sample was not adequately powered to evaluate interactions between Aβ and APOE4, exploratory analyses examined differences by APOE4 stratified by Aβ status. Analyses were repeated within the CN subgroup to assess differences by APOE4 and Aβ among asymptomatic individuals, and exploratory analyses assessed differences by cognitive status (CN/CI).

To evaluate localized associations between BBB permeability and microstructure, for each region of interest, linear regressions were performed with K_{trans} as the regressor, RSI metric as the outcome, and covariates of age, sex, and scanner software version. To assess whether APOE4 or Aβ modified associations between BBB permeability and microstructure, regressions were repeated with an interaction term between mean-centered K_{trans} and APOE4 or Aβ. Regressions demonstrating interactions were followed by models stratified by APOE4 or Aβ. Regressions were conducted across the full sample and within CN individuals.

To determine whether BBB permeability was associated with macroscopic measures of neurodegeneration, regressions (adjusted for age and sex) were conducted with K_{trans} as the regressor and cortical thickness or volume of the hippocampus or white matter (corrected for intracranial volume) as the outcome. To test whether atrophy contributed to the results, analyses showing significant effects were repeated adjusting for the respective thickness or volumetric measure in that region.

3 | RESULTS

3.1 | Participant characteristics

Participant characteristics by cognitive status are shown in Table 1. As expected, CI scored lower on the MMSE than CN ($F(1,50) = 5.88$, $p = 0.02$) and were more likely to be amyloid-positive ($x^2(1) = 4.70$, $p = 0.03$), but CI and CN participants did not differ on age, sex, education, or APOE4 carriage. Participant characteristics did not differ by APOE4 status among the full sample or CN (Table S1). Participants were 95% non-Hispanic White and 4% Asian (one participant declined disclosure).

3.2 | Associations of BBB permeability with participant demographics

K_{trans} neither correlated with age or education ($p > 0.05$) nor differed between men and women (adjusted for age, $p > 0.05$; Table S2, Figure S1), although there was a trend toward higher hippocampal K_{trans} for women than men ($p = 0.09$).

3.3 | Associations of BBB permeability with Aβ and cognition

K_{trans} did not differ by Aβ status ($p > 0.05$, adjusted for age and sex), although there was a trend toward higher parahippocampal K_{trans} for amyloid-positive participants ($p = 0.06$; Table S3, Figure S2). Linear regressions revealed no association between K_{trans} and performance on any cognitive test ($p > 0.05$, adjusted for age, sex, and education; Table S4). Exploratory analyses showed no differences in K_{trans} by diagnosis ($p > 0.30$, adjusted for age and sex; Table S5, Figure S3).
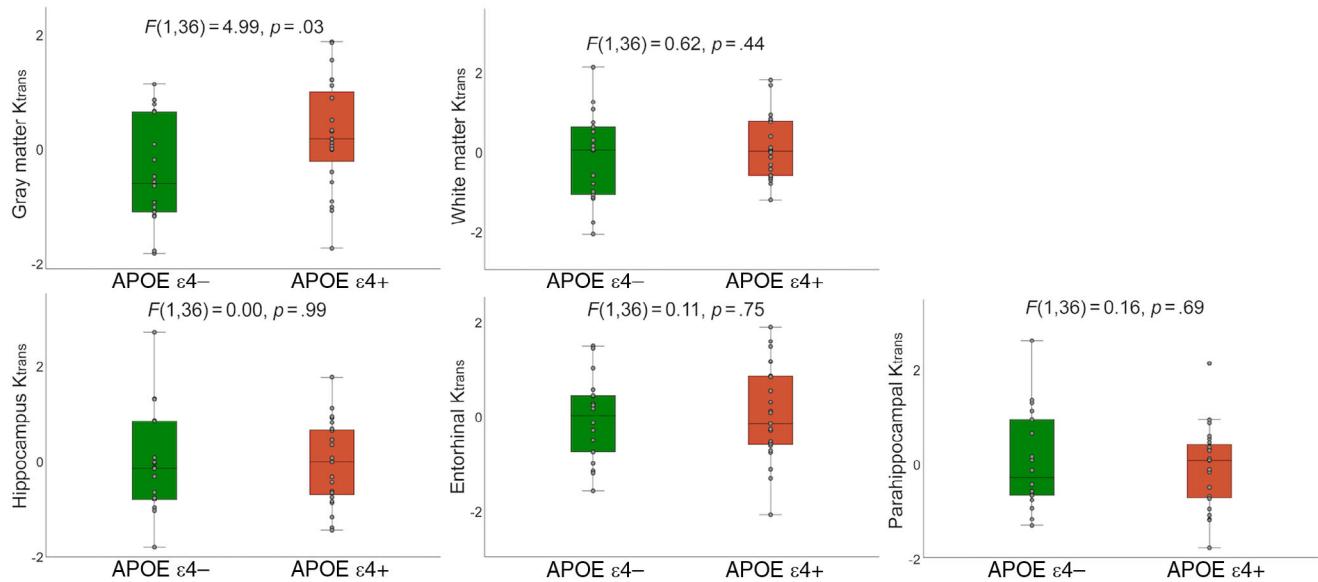
FIGURE 1 Differences in K_{trans} by *APOE4*. K_{trans} for *APOE4* carriers ($N = 23$) and non-carriers ($N = 18$) are shown for CN participants. Values represent standardized residuals, adjusted for age, sex, and Aβ using linear regression. CN, cognitively normal.

3.4 | Differences in BBB permeability by APOE4

Across all participants, there was a trend toward higher gray matter K_{trans} in *APOE4* carriers compared to non-carriers (adjusted for age and sex; $F(1,51) = 2.73$, $p = 0.10$) that reached significance after further adjustment for Aβ ($F(1,45) = 4.71$, $p = 0.04$; Table S6). This difference persisted within the CN subgroup ($F(1,36) = 4.99$, $p = 0.03$; Figure 1) and was unchanged after further adjustment for gray matter thickness (full sample: $F(1,44) = 4.62$, $p = 0.04$; CN: $F(1,35) = 5.11$, $p = 0.03$). Exploratory amyloid-stratified analyses revealed that gray matter K_{trans} was elevated for *APOE4* carriers among amyloid-negative CN ($F(1,11) = 5.14$, $p = 0.04$, Figure S4), with no difference by *APOE4* for amyloid-positive CN ($F(1,22) = 1.24$, $p = 0.28$).

3.5 | Associations between BBB permeability and brain microstructure

To examine whether BBB permeability was related to brain microstructure, linear regressions (adjusted for age, sex, and scanner software; standardized β values are reported) assessed associations between K_{trans} and RSI metrics within the corresponding region. Higher entorhinal K_{trans} was associated with higher entorhinal free water across the full sample ($\beta = 0.28$, $p = 0.02$) and within the CN subgroup ($\beta = 0.34$, $p = 0.009$), with trends toward associations with lower restricted isotropic, neurite density, and hindered diffusion (Table 2). K_{trans} was not associated with cortical thickness or volume in any region (Table S7), and the association with entorhinal free water was unchanged after further adjustment for entorhinal cortex thickness (full sample: $\beta = 0.17$, $p = 0.03$; CN: $\beta = 0.20$, $p = 0.04$). K_{trans} was not associated with brain microstructure in any other region (Table S8).

Among CN participants, Aβ status interacted with entorhinal K_{trans} on entorhinal microstructure (Table S9), with amyloid-stratified analyses indicating associations of higher K_{trans} with lower restricted isotropic diffusion ($\beta = -0.25$, $p = 0.02$; interaction $\beta = -0.19$, $p = 0.02$), lower neurite density ($\beta = -0.52$, $p = 0.003$; interaction $\beta = -0.43$, $p = 0.002$) and higher free water ($\beta = 0.56$, $p = 0.003$; interaction $\beta = 0.29$, $p = 0.03$) only for amyloid-positive individuals (Figure 2A). *APOE4* interacted with entorhinal K_{trans} for entorhinal free water ($\beta = 0.32$, $p = 0.01$), with *APOE4*-stratified regressions demonstrating that associations were present only for *APOE4* carriers ($\beta = 0.58$, $p = 0.001$; Table S10; Figure 2B). Although we were not adequately powered to assess three-way interactions among K_{trans}, *APOE4*, and Aβ, exploratory analyses revealed that the associations of entorhinal K_{trans} with entorhinal microstructure were generally stronger among amyloid-positive *APOE4* carriers and weakest among amyloid-negative *APOE4* non-carriers (Figure S5).

4 | DISCUSSION

Integrating a multimodal DCE and diffusion MRI approach with Aβ and genetic characterization, this study evaluated competing hypotheses that BBB breakdown in early AD is localized to medial temporal targets of AD-related neurodegeneration or is a widespread, whole-brain phenomenon. Global cortical gray matter BBB leakage was observed among CN amyloid-negative *APOE4* carriers, supporting the latter hypothesis, but did not materially differ by cognitive impairment. BBB permeability correlated with entorhinal microstructural abnormalities, with associations specific to *APOE4* carriers and amyloid-positive individuals, providing novel evidence that neurovascular dysfunction may interact with AD pathophysiology to accelerate regional neurodegeneration.

TABLE 2 Linear regression model results (standardized β, p value) for associations between entorhinal K_{trans} and entorhinal microstructure, among all participants and within cognitive participants.

	Restricted isotropic	Neurite density	Hindered	Free water
ALL				
Age	$\beta = -0.09\, p = 0.19$	$\beta = -0.42\, p < 0.001$	$\beta = -0.27\, p = 0.03$	$\beta = 0.39\, p = 0.002$
Sex	$\beta = -0.07\, p = 0.33$	$\beta = -0.14\, p = 0.23$	$\beta = -0.29\, p = 0.02$	$\beta = 0.29\, p = 0.02$
Scanner software	$\beta = 0.85\, p < 0.001$	$\beta = 0.36\, p = 0.002$	$\beta = -0.38\, p = 0.002$	$\beta = 0.02\, p = 0.88$
K_{trans}	$\beta = -0.14\, p = 0.05$	$\beta = -0.21\, p = 0.06$	$\beta = -0.18\, p = 0.14$	$\beta = 0.28\, p = 0.02$
COGNITIVELY				
Age	$\beta = -0.07\, p = 0.38$	$\beta = -0.43\, p = 0.001$	$\beta = -0.21\, p = 0.10$	$\beta = 0.37\, p = 0.006$
NORMAL				
Sex	$\beta = -0.07\, p = 0.36$	$\beta = -0.18\, p = 0.17$	$\beta = -0.31\, p = 0.02$	$\beta = 0.35\, p = 0.01$
Scanner software	$\beta = 0.86\, p < 0.001$	$\beta = 0.34\, p = 0.01$	$\beta = -0.49\, p < 0.001$	$\beta = 0.09\, p = 0.48$
K_{trans}	$\beta = -0.13\, p = 0.11$	$\beta = -0.22\, p = 0.08$	$\beta = -0.21\, p = 0.08$	$\beta = 0.34\, p = 0.009$

Bold indicates significant ($p < 0.05$).
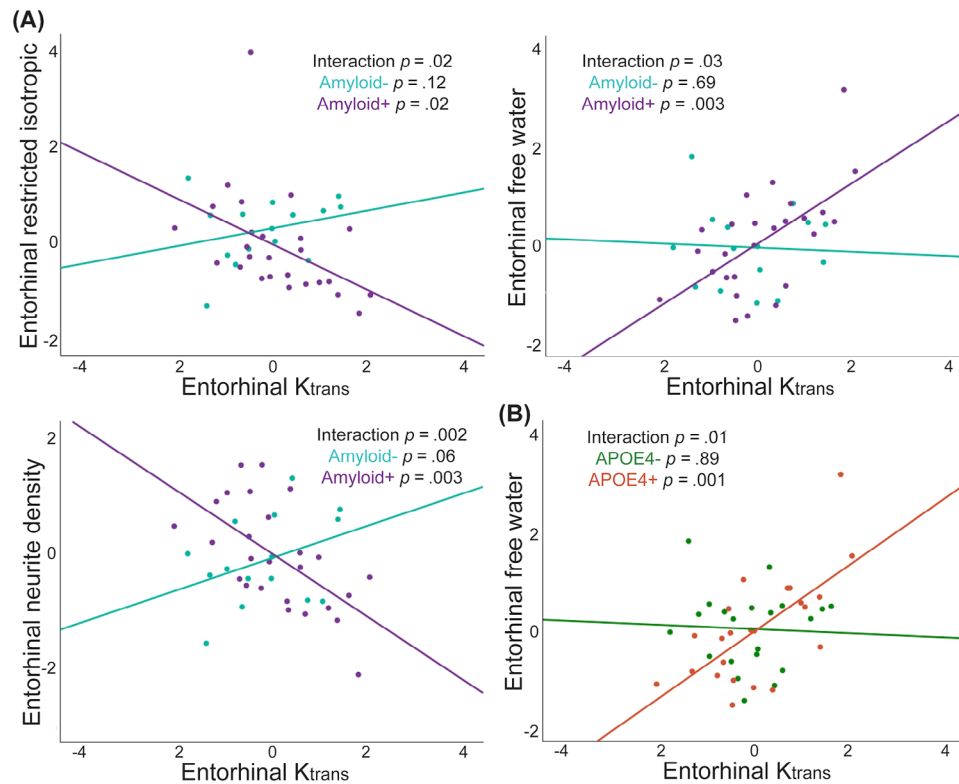
FIGURE 2 Interactions of K_{trans} with *APOE4* and Aβ on entorhinal microstructure. Associations of entorhinal K_{trans} with entorhinal microstructure demonstrating significant interactions with (A) Aβ (amyloid-negative $N = 15$; amyloid-positive $N = 26$) or (B) *APOE4* (*APOE4* non-carrier $N = 21$; *APOE4* carrier $N = 23$) are shown for CN participants. Values represent standardized residuals, adjusted for age, sex, and scanner software, using linear regression. CN, cognitively normal.

Extending recent evidence that *APOE4* compromises BBB integrity,[12,13] we report elevated cortical gray matter BBB permeability in *APOE4* carriers, independent of cortical atrophy. Critically, this difference manifested both among the full sample representing the spectrum from CN to mildly impaired and within CN amyloid-negative individuals, suggesting that widespread *APOE4*-dependent BBB dysfunction emerges early along the AD continuum before detectable Aβ accumulation or neurodegeneration. Indeed, BBB permeability did

not differ by diagnosis or correlate with cognitive function, suggesting that primary BBB disruption may manifest in preclinical stages and minimally progress with cognitive decline. Age was not associated with BBB permeability, supporting recent consensus that substantial BBB disruption does not reliably occur in normal aging,[1] but more likely reflects underlying pathophysiology. Although our findings conflict with reports of increased permeability with cognitive impairment,[6] they align with more recent evidence for BBB leakage in *APOE4* carriers but not in MCI,[13] and that BBB permeability does not differ between MCI and AD dementia.[11] However, our failure to detect BBB leakage with cognitive impairment may be attributable to our small CI sample or to a high proportion of preclinical AD among our CN sample, which was highly enriched for *APOE4* and amyloid positivity, thus minimizing differences with the mildly impaired CI group.

We were unable to replicate reports of *APOE4*-dependent BBB breakdown within the medial temporal lobe[6,13] but rather observed diffusely distributed cortical gray matter BBB leakage among *APOE4* carriers. Our findings extend evidence from van de Haar et al.[11] for BBB breakdown across cortical gray matter in MCI. Methodological differences or variability in cohort characteristics may account for inconsistencies across studies, warranting further investigation into both the topography and temporal dynamics of BBB breakdown along the AD continuum.

We provide novel evidence that BBB breakdown in the entorhinal cortex is associated with microstructural abnormalities that are modified by Aβ and *APOE4* and not accounted for by atrophy. Entorhinal BBB permeability correlated with higher free water across the full sample, which was driven by CN *APOE4* carriers. Amyloid-positive CN individuals also exhibited associations of entorhinal BBB leakage with lower restricted diffusion and neurite density and higher free water, with the strongest correlations among amyloid-positive *APOE4* carriers. Thus, while *APOE4*-related BBB leakage may be regionally nonspecific, for *APOE4* carriers harboring preclinical AD pathology, BBB breakdown within the entorhinal cortex, a site of early AD-related neurodegeneration, may elicit subtle cytoarchitectural changes, including neurite loss and expansion of the CSF compartment. In a partially overlapping sample (85% independent), we previously reported reduced entorhinal neurite density in CN *APOE4* carriers.[35] Here, we extend this evidence to suggest that cerebrovascular dysfunction synergistic with AD pathogenic changes may lie upstream of preclinical neurodegeneration in the entorhinal cortex among *APOE4* carriers. Given the vulnerability of the entorhinal cortex to Braak stage I tau, further investigation is warranted to interrogate interactions with tau for which biomarkers were unavailable in this dataset. Both *APOE4* and tau have been linked to tight junction loss[36]; tau can induce vessel abnormalities and BBB dysfunction,[37,38] and *APOE4* promotes tau pathogenesis and neurodegeneration.[39] Moreover, *APOE4* can activate microglia and promote inflammation,[14] which can drive BBB dysfunction[15] as well as tau hyperphosphorylation and propagation.[40] Though speculative, one explanation integrating this evidence is that widespread *APOE4*-dependent BBB dysfunction occurs before substantial AD pathological burden, which in the subsequent company of Aβ and perhaps a hyperinflammatory environment may accelerate the translation of BBB breakdown to neurodegeneration in tau-vulnerable regions.[39] Our findings further highlight the need to understand potential neurodegenerative sequelae of BBB dysfunction related to anti-Aβ immunotherapy, which is associated with amyloid-related imaging abnormalities (ARIA) of presumed vascular origin in an *APOE4* dose-dependent manner.

Although this study was not powered to examine sex differences, there was a pattern of elevated hippocampal BBB permeability for women versus men. Further research is needed to characterize sex differences in BBB breakdown along the AD continuum, which may be affected by differences in factors such as neurovascular integrity and signaling, cardiovascular function,[41] immune signaling,[42] lifestyle factors such as diabetes, obesity, or sleep disorders,[43,44] or declining neuroprotective effects of estrogen[45] with menopause.

The cross-sectional, observational design of this study precluded inferring temporal dynamics of BBB dysfunction along the AD continuum or underlying mechanisms. The limited number of amyloid PET scans and the unavailability of a tau biomarker prevented the examination of topographic colocalization of BBB permeability with AD pathology. Furthermore, the use of multiple methods to determine amyloid positivity may have introduced variability into our analyses of amyloid status, although all PET and biofluid markers were well-validated in independent cohorts. Finally, our mostly well-educated, non-Hispanic White sample was relatively homogeneous in terms of race/ethnicity and socioeconomic status. Future longitudinal investigations with multimodal biomarker assessment among more diverse and representative populations are needed to improve generalizability.

In conclusion, *APOE4* may promote widespread cortical BBB breakdown in preclinical AD before the accumulation of detectable Aβ pathology. This BBB dysfunction is associated with deleterious cytoarchitectural changes in AD-vulnerable regions, particularly in the presence of Aβ. These findings support mounting evidence for neurovascular dysfunction as a significant contributor to AD pathogenesis and for *APOE* as a candidate preclinical therapeutic target for arresting cerebrovascular damage that may accelerate neurodegeneration.

CONFLICT OF INTEREST STATEMENT

The authors report no competing interests. Author disclosures are available in the Supporting Information.

CONSENT STATEMENT

Study procedures were approved by the University of California, San Diego Human Research Protections Program Board, and participants provided informed written consent before participation.

ORCID

Emilie T. Reas https://orcid.org/0000-0002-4110-5154

REFERENCES

1. Banks WA, Reed MJ, Logsdon AF, Rhea EM, Erickson MA. Healthy aging and the blood-brain barrier. *Nat Aging*. 2021;1:243-254.
2. Sweeney MD, Sagare AP, Zlokovic BV. Blood-brain barrier breakdown in Alzheimer disease and other neurodegenerative disorders. *Nat Rev Neurol*. 2018;14:133-150.
3. Janelidze S, Hertze J, Nägga K, et al. Increased blood–brain barrier permeability is associated with dementia and diabetes, but not amyloid pathology or APOE genotype. *Neurobiol Aging*. 2017;51:104-112.
4. Sweeney MD, Montagne A, Sagare AP, et al. Vascular dysfunction-The disregarded partner of Alzheimer's disease. *Alzheimers Dement*. 2019;15:158-167.
5. Andjelkovic AV, Situ M, Citalan-Madrid AF, Stamatovic SM, Xiang J, Keep RF. Blood–brain barrier dysfunction in normal aging and neurodegeneration: mechanisms, impact, and treatments. *Stroke*. 2023;54:661-672.
6. Nation DA, Sweeney MD, Montagne A, et al. Blood-brain barrier breakdown is an early biomarker of human cognitive dysfunction. *Nat Med*. 2019;25:270-276.
7. Miners JS, Kehoe PG, Love S, Zetterberg H, Blennow K. CSF evidence of pericyte damage in Alzheimer's disease is associated with markers of blood–brain barrier dysfunction and disease pathology. *Alzheimers Res Ther*. 2019;11:81.
8. Halliday MR, Pomara N, Sagare AP, Mack WJ, Frangione B, Zlokovic BV. Relationship between cyclophilin A levels and matrix metalloproteinase 9 activity in cerebrospinal fluid of cognitively normal apolipoprotein E4 carriers and blood-brain barrier breakdown. *JAMA Neurol*. 2013;70:1198-1200.
9. Karch A, Manthey H, Ponto C, et al. Investigating the association of APOE genotypes with blood–brain barrier dysfunction measured by cerebrospinal fluid-serum albumin ratio in a cohort of patients with different types of dementia. *PLoS One*. 2013;8:e84405.
10. Montagne A, Barnes SR, Sweeney MD, et al. Blood-brain barrier breakdown in the aging human hippocampus. *Neuron*. 2015;85:296-302.
11. van de Haar HJ, Burgmans S, Jansen JF, et al. Blood–brain barrier leakage in patients with early Alzheimer's disease. *Radiology*. 2016;281:527-535.
12. Montagne A, Nation DA, Sagare AP, et al. APOE4 leads to blood–brain barrier dysfunction predicting cognitive decline. *Nature*. 2020;581:71-76.
13. Moon W-J, Lim C, Ha IH, et al. Hippocampal blood-brain barrier permeability is related to the APOE4 mutation status of elderly individuals without dementia. *J Cereb Blood Flow Metab*. 2021;41:1351-1361.
14. Krasemann S, Madore C, Cialic R, et al. The TREM2-APOE pathway drives the transcriptional phenotype of dysfunctional microglia in neurodegenerative diseases. *Immunity*. 2017;47:566-581. e9.
15. Bell RD, Winkler EA, Singh I, et al. Apolipoprotein E controls cerebrovascular integrity via cyclophilin A. *Nature*. 2012;485:512-516.
16. Alata W, Ye Y, St-Amour I, Vandal M, Calon F. Human Apolipoprotein E ε4 expression impairs cerebral vascularization and blood—brain barrier function in mice. *J Cereb Blood Flow Metab*. 2015;35:86-94.
17. Huynh TV, Davis AA, Ulrich JD, Holtzman DM. Apolipoprotein E and Alzheimer's disease: the influence of apolipoprotein E on amyloid-beta and other amyloidogenic proteins. *J Lipid Res*. 2017;58:824-836.
18. Nishitsuji K, Hosono T, Nakamura T, Bu G, Michikawa M. Apolipoprotein E regulates the integrity of tight junctions in an isoform-dependent manner in an in vitro blood–brain barrier model. *J Biol Chem*. 2011;286:17536-17542.
19. Montagne A, Zhao Z, Zlokovic BV. Alzheimer's disease: a matter of blood–brain barrier dysfunction?. *J Exp Med*. 2017;214:3151-3169.
20. Skillbäck T, Blennow K, Zetterberg H, et al. Sex differences in CSF biomarkers for neurodegeneration and blood–brain barrier integrity. *Alzheimers Dement (Amst)*. 2021;13:e12141.
21. Galasko D, Hansen LA, Katzman R, et al. Clinical-Neuropathological correlations in Alzheimer's disease and related dementias. *Arch Neurol*. 1994;51:888-895.
22. Xiao MF, Xu D, Craig MT, et al. NPTX2 and cognitive dysfunction in Alzheimer's disease. *eLife*. 2017;6:e23798.
23. Vanderstichele H, Bibl M, Engelborghs S, et al. Standardization of preanalytical aspects of cerebrospinal fluid biomarker testing for Alzheimer's disease diagnosis: a consensus paper from the Alzheimer's Biomarkers Standardization Initiative. *Alzheimers Dement*. 2012;8:65-73.
24. Janelidze S, Zetterberg H, Mattsson N, et al. CSF Abeta42/Abeta40 and Abeta42/Abeta38 ratios: better diagnostic markers of Alzheimer disease. *Ann Clin Transl Neurol*. 2016;3:154-165.
25. Dage JL, Russ KA, Kostadinova RV, et al. Assigning and monitoring performance of cut points for Plasma P-tau181 for use in prospective studies. International Conference on Alzheimer's and Parkinson's diseases and Related Neurological Disorders, Lisbon, Portugal, 5-9 March 2024. Alzheimer's disease International; 2024.
26. Salmon D, Butters N. Neuropsychological assessment of dementia in the elderly. *Principles Geriatr Neurol*. 1992;144:63.
27. Hagler DJ Jr, Hatton S, Cornejo MD, et al. Image processing and analysis methods for the Adolescent Brain Cognitive Development study. *Neuroimage*. 2019;202:116091.
28. Jenkinson M, Beckmann CF, Behrens TEJ, Woolrich MW, Smith SM. FSL. *Neuroimage*. 2012;62:782-790.
29. Fischl B, Salat DH, Busa E, et al. Whole brain segmentation: automated labeling of neuroanatomical structures in the human brain. *Neuron*. 2002;33:341-355.
30. Hagler DJ, Jr., Ahmadi ME, Kuperman J, et al. Automated white-matter tractography using a probabilistic diffusion tensor atlas: application to temporal lobe epilepsy. *Hum Brain Mapp*. 2009;30:1535-1547.
31. Barnes SR, Ng TS, Santa-Maria N, Montagne A, Zlokovic BV, Jacobs RE. ROCKETSHIP: a flexible and modular software tool for the planning, processing and analysis of dynamic MRI studies. *BMC Med Imaging*. 2015;15:19.
32. Heye AK, Thrippleton MJ, Armitage PA, et al. Tracer kinetic modelling for DCE-MRI quantification of subtle blood-brain barrier permeability. *Neuroimage*. 2016;125:446-455.
33. Ewing JR, Knight RA, Nagaraja TN, et al. Patlak plots of Gd-DTPA MRI data yield blood–brain transfer constants concordant with those of 14C-sucrose in areas of blood-brain opening. *Magn Reson Med*. 2003;50:283-292.
34. White NS, Leergaard TB, D'Arceuil H, Bjaalie JG, Dale AM. Probing tissue microstructure with restriction spectrum imaging: histological and theoretical validation. *Hum Brain Mapp*. 2013;34:327-346.
35. Reas ET, Triebswetter C, Banks SJ, McEvoy LK. Effects of APOE2 and APOE4 on brain microstructure in older adults: modification by age, sex, and cognitive status. *Alzheimers Res Ther*. 2024;16:7.
36. Liu C-C, Yamazaki Y, Heckman MG, et al. Tau and apolipoprotein E modulate cerebrovascular tight junction integrity independent of cerebral amyloid angiopathy in Alzheimer's disease. *Alzheimers Dement*. 2020;16:1372-1383.
37. Blair LJ, Frauen HD, Zhang B, et al. Tau depletion prevents progressive blood–brain barrier damage in a mouse model of tauopathy. *Acta Neuropathol Commun*. 2015;3:8.
38. Bennett RE, Robbins AB, Hu M, et al. Tau induces blood vessel abnormalities and angiogenesis-related gene expression in P301L transgenic mice and human Alzheimer's disease. *Proc Natl Acad Sci*. 2018;115:E1289-E1298.
39. Shi Y, Yamada K, Liddelow SA, et al. ApoE4 markedly exacerbates tau-mediated neurodegeneration in a mouse model of tauopathy. *Nature*. 2017;549:523-527.

40. Leyns CEG, Holtzman DM. Glial contributions to neurodegeneration in tauopathies. *Mol Neurodegener*. 2017;12:50.

41. Ji H, Kwan AC, Chen MT, et al. Sex differences in myocardial and vascular aging. *Circ Res*. 2022;130:566-577.

42. Klein SL, Flanagan KL. Sex differences in immune responses. *Nat Rev Immunol*. 2016;16:626-638.

43. Lok R, Qian J, Chellappa SL. Sex differences in sleep, circadian rhythms, and metabolism: implications for precision medicine. *Sleep Med Rev*. 2024;75:101926.

44. Meyer MR, Clegg DJ, Prossnitz ER, Barton M. Obesity, insulin resistance and diabetes: sex differences and role of oestrogen receptors. *Acta Physiol*. 2011;203:259-269.

45. Maggioli E, McArthur S, Mauro C, et al. Estrogen protects the blood–brain barrier from inflammation-induced disruption and increased lymphocyte trafficking. *Brain Behav Immun*. 2016;51:212-222.

SUPPORTING INFORMATION

Additional supporting information can be found online in the Supporting Information section at the end of this article.